ChemComm

COMMUNICATION

Cite this: DOI: 10.1039/c7cc04346e

Received 5th June 2017,
Accepted 10th August 2017

DOI: 10.1039/c7cc04346e

rsc.li/chemcomm

Thermo-mechanically responsive crystalline organic cantilever†

Madushani Dharmarwardana,[a] Raymond P. Welch,[a] Sunah Kwon,[b] Victoria K. Nguyen,[a] Gregory T. McCandless,[a] Mohammad A. Omary[c] and Jeremiah J. Gassensmith*[a]

We report thermo-mechanically responsive and thermochromic behavior in the single crystalline organic semiconductor butoxyphenyl *N*-substituted naphthalene diimide (BNDI). We show that initially monoclinic single crystals of BNDI undergo a single-crystal to single-crystal transition to a triclinic phase. This transition accompanies large changes in the crystal packing, a visible decrease in crystal size, reversible thermochromic behavior, and motion including bending, jumping, and splitting. We have shown that by fixing single crystals to a surface, we can harness the energy of the phase transition to create a single crystal cantilever capable of lifting weights with masses nigh two orders of magnitude heavier than the single crystal itself.

Kinetic stimuli responsive behavior—the ability to move in response to the input of energy from an external source—has been engineered in a wide range of flexible materials from bulk polymers[1–7] to viral nanoparticles.[8–10] These soft materials readily undergo chemical functionalization and stimuli responsiveness can be straightforward to introduce.[1] Finding such a motion in highly crystalline solids is still unusual and surprising.[11,12] That said, recent examples of single crystals that bend, jump,[13,14] split,[15,16] coil,[17] and explode[18] when prodded into undergoing either a phase transition or topochemical reaction[19–23] have emerged in the literature. This rapid and controllable dynamic behavior has attracted some interest owing to potential applications such as micron or nanoscale actuators for smart medical devices, artificial muscles, sensors, and memory devices.[12,24–27] In most cases, this induced motion leads to disintegration after the phase transition; thus, such crystals are not suitable for structure determination following actuation. In contrast, only a few examples[14–29] of organic molecular crystals showing thermo-mechanical single crystal-to-single crystal (SC–SC) transitions have been reported. Donor–acceptor stacks containing electron deficient naphthalene diimide subunits and electron rich dialkoxynaphthalene subunits have been shown to undergo phase transitions in response to temperature changes—giving rise to thermochromism.[28] What remains unclear is whether this thermal responsiveness is a general phenomenon to planar aromatics or whether it is unique to donor–acceptor systems.[29–31] In other words, we wondered if a similar thermo-responsive behavior could be achieved with just a single type of subunit—either single crystals containing only an electron donor or an electron acceptor. In the course of this study, we discovered that the monoclinic polymorph (α-phase) of single crystals containing exclusively butoxyphenyl *N*-substituted naphthalene diimide (BNDI) (Fig. 1a) not only undergoes significant intermolecular changes in stacking distance, but also, when heated, undergoes a thermo-mechanical responsive SC–SC change to a reversibly thermochromic triclinic (β-phase) system.

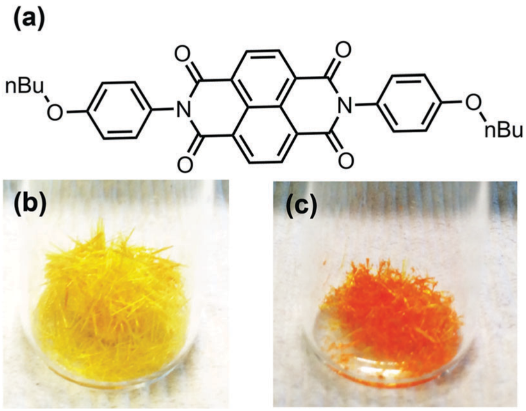

Fig. 1 (a) Chemical structure of BNDI; photographs of polymorphs: the (b) non-thermochromic α-phase and the (c) thermochromic β-phase.

---

[a] *Department of Chemistry and Biochemistry, University of Texas at Dallas, 800 West Campbell Road, Richardson, TX 75080-3021, USA. E-mail: gassensmith@utdallas.edu*
[b] *Department of Material Science and Engineering, University of Texas at Dallas, 800 West Campbell Road, Richardson, TX 75080-3021, USA*
[c] *Department of Chemistry, University of North Texas, 1155 Union Circle, Denton, TX 76203, USA*

† Electronic supplementary information (ESI) available: Experimental details, single crystal X-ray data, NMR spectra, DSC curves and Movies S1–S10. CCDC 1497523 and 1497526. For ESI and crystallographic data in CIF or other electronic format see DOI: 10.1039/c7cc04346e

This is made all the more interesting because naphthalene diimide structures are one of only a handful of n-type organic semiconductors[32] and BNDI is known to have n-type semiconducting properties[32,33] in the solid state. Intriguingly, the concurrent existence of polymorphism[34] and thermo-mechanical behavior in the solid state have yet to be reported for any naphthalene diimide—or any perylene derivative for that matter—despite several examples of liquid crystalline systems[35–37] and polymers[38] of these materials showing such behavior.[39] During our initial investigation of BNDI single crystals, we found we could induce the quantitative growth of two phase-pure BNDI derivatives by changing the solution growth conditions. Specifically, we found the known yellow monoclinic polymorph (α-phase shown in Fig. 1b), which we initially believed to be thermally inert based on temperature dependent single crystal X-ray diffraction (SXRD) experiments and a thermochromic triclinic polymorph (β-phase), which produces orange crystals at room temperature (Fig. 1c). While testing the presumed ''thermal-inertness'' of the yellow α-phase crystals, we discovered that, after heating to around 400 K and then upon cooling, the crystals became orange and displayed identical thermochromic behavior as that for the triclinic β-phase. We suspected that the crystals interconverted between the two polymorphs, which would have been surprising given the large difference in unit cell parameters (Table S1, ESI†).

In most reported cases, thermo-mechanically responsive molecular crystals are isosymmetric after the phase transition and only minor changes of the unit cell are noted.[40–44] In the instance of BNDI, however, crystal symmetry is not preserved and a comparatively massive change in the unit cell is observed. Fig. 2, for instance, shows both polymorphs along the crystallographic *a*-axis and clearly illustrates these large anisotropic changes in packing. We witnessed this first-hand when a single crystal of the monoclinic α-phase was evaluated by SXRD analysis at room temperature. The crystal was then heated in a round bottom flask using an oil bath to around 400 K, cooled down to 90 K, and SXRD data were collected. The thermally transformed polymorph, now in the β-phase, continued to diffract, though with some attenuation in long range order (Fig. S3 and Table S1, ESI†) and the emergence of disorder presumed to be associated with twinning. Frequently, we found that the crystals would undergo even more extreme motion; for instance, rapid vibration and jumping were seen, though, about 75% of the time, the crystals would bend out of plane (Fig. S4–S8, ESI†).

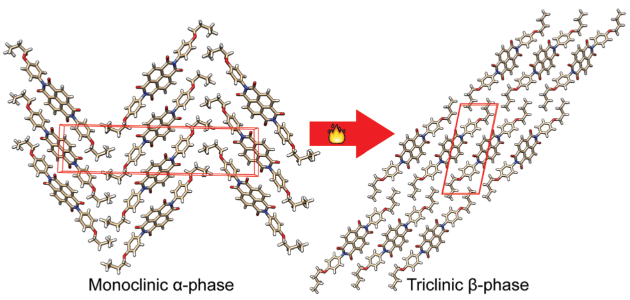

Fig. 2 Perspective projections of the crystallographic packing in the SC–SC transition from the monoclinic α-phase to the triclinic β-phase. Upon heat treatment, the crystal lattice changes from herringbone packing to infinite 1D chains stacked co-facially along their π surfaces. The red box represents the unit cells of the respective crystals. Both images are oriented along the crystallographic *a*-axis.

We characterized this dynamic behavior using hot-stage microscopy to analyze the morphological and color changes of the α-phase during this anomalous transition. When millimeter-sized single crystals in the α-phase were heated on the stage of a polarized optical microscope, the crystal initially expanded, but no movement was observed until the temperature reached around 400 K. At that point, a clear ''wave front'' began at one extreme end of a crystal and propagated to the other end followed by a change from bright yellow to dark yellow (Fig. 3 and Movie S1, ESI†). At this point the crystal started showing movements such as cracking, splitting, jumping, and bending (Fig. S6–S9 and Movies S1, S2, ESI†). If the crystal did not jump out of view, we could then lower the temperature of the stage. Once the crystals underwent a transformation to the thermochromic β-phase, they changed color to red/orange as the stage was reduced to cryogenic temperatures (Fig. 3).

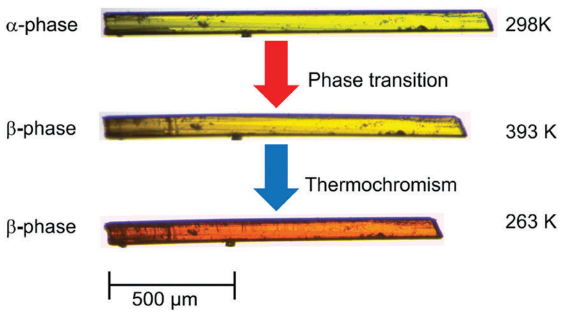

Fig. 3 Changes of crystal dimensions during the α-phase to the β-phase transformation.

While most of the crystals ended up irreversibly bending during the phase transition, some crystals of the α-phase were either much less dramatic in movement (Fig. S10, ESI†) or bent back into plane following the transition. This allowed us to record the contraction of a crystal while it was heated beyond the phase transition and then cooled. The crystal contracted approximately 5% following the phase transition and a further 13% upon cooling to 263 K (Tables S2, S3 and Fig. S4, ESI†, and Fig. 3). From our SXRD data it is clear that the transition from α-phase to β-phase results in a radically different unit cell and it is quite clear the crystals themselves change in size.

Whilst the dynamic behavior we describe here is uncommon, several elegant studies[13,16,18,41–43,45–47] have postulated that the stress accumulation within the crystal due to the molecular rearrangement is transformed into mechanical force. We sought to quantify this mechanical force, at least rudimentarily, by converting the single crystals into molecular single crystal cantilevers. To do this, we glued one end of the crystal to the surface of a glass cover slip and a metal ball was loaded onto the other end of the crystal (Fig. 4). The coverslip was then placed

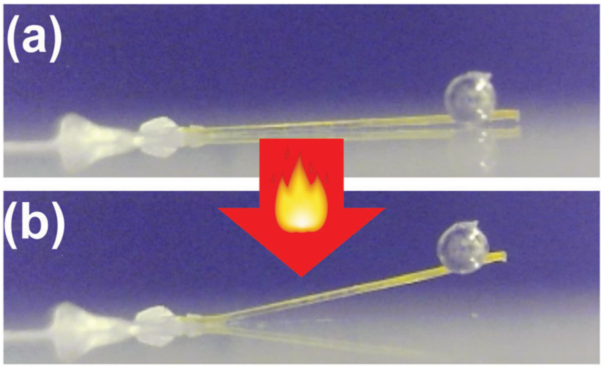

Fig. 4 Thermo-mechanical work of a BNDI cantilever. (a) Before the phase transition. (b) After the phase transition. The crystal was heated on a glass slide on the heating stage of a polarized optical microscope. The mass of the crystal and a 0.5 mm diameter tungsten carbide ball is 0.0100 mg and 0.8320 mg, respectively.

onto a heated stage and we recorded its behavior as the temperature passed and then retreated from the phase transition temperature. We tried a range of crystal sizes and two sizes of metal balls to quantify the thermo-mechanical behaviour of this unique system (Table S4, Fig. S12–S16, and Movies S4–S10, ESI†). The maximum load we were able to lift with 3.5 mm long BNDI crystal was a 4.113 mg stainless steel metal ball to a height of 0.24 mm (Fig. S15 and Movie S7, ESI†). In this case, the metal ball is 91 times heavier than the BNDI crystal, the amount of work done by the BNDI cantilever is about 0.01 μJ, and the force generated from the α-phase to the β-phase transition is 40 μN.

Differential scanning calorimetry (DSC) analysis on bulk samples of the yellow monoclinic α-phase had yet another surprise in store for us—a second transition at an even higher temperature. The DSC scans shown in Fig. 5a reveal the multiple phase transitions: (1) the expected transition from the α-phase to the β-phase at 388 K; (2) followed by a transition to a new γ-phase at 479 K; and (3) a return to the β-phase upon cooling below 408 K. When this thermal cycle is repeated on the same sample, only the transition between the β-phase and γ-phase is observed, indicating that this transition is reversible. The DSC data of both polymorphs clearly indicated that this phase transition is transforming the α-phase to a more thermodynamically stable and highly thermochromic β-phase (Fig. 5b and Fig. S17, ESI†). During the β-phase to γ-phase transformation, the crystals lose some of their crystallinity, which results in the peak shifting in the second heating cycle (Fig. 5a).[48,49]

We confirmed the bulk material underwent reversible crystallographic phase transitions using variable temperature powder X-ray diffraction (PXRD). As shown in Fig. 5b, as the temperature increases on a sample of pure α-phase BNDI, the reflections of the α-phase peaks decrease and a new set of reflections corresponding to the β-phase appears. As we further increase the temperature, the α-phase completely transforms to the β-phase, which then gives way to the γ-phase at temperatures above 480 K. As we cool down the sample to room temperature, the intensity of the β-phase peaks increases and the γ-phase completely disappears. Thus far, we have been unable to obtain SXRD data of this high temperature γ-phase, as the single crystals become polycrystalline. Curiously, at these high temperatures, the β-phase is bright yellow. Once it enters the γ-phase, it suddenly becomes orange, indicating that the packing conformation has clearly changed into something quite distinct. Notably, upon cooling, the crystals again turn yellow at the phase transition and then are again thermochromic, and they still strongly diffract by PXRD.[50]

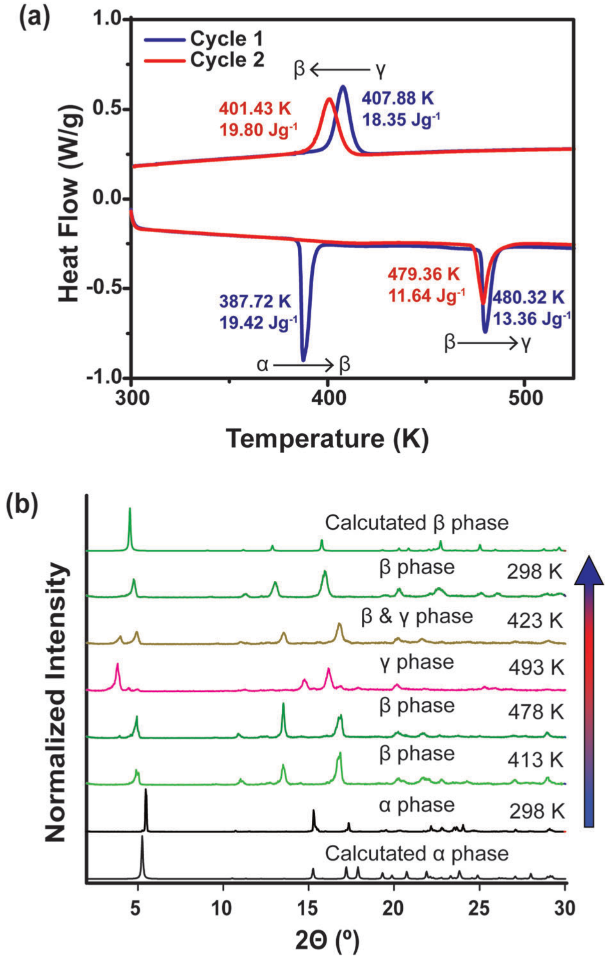

Fig. 5 (a) DSC curves for the α-phase; heating rate is 10 K min^{-1} (b) variable temperature PXRD data for the α-phase.

In summary, we have demonstrated the SC–SC polymorphic transition of the α-phase of the organic semiconductor BNDI to its highly thermochromic β-phase followed by a reversible polymorphic transition to a γ-phase, which only exists at high temperatures. During the polymorphic α-phase to β-phase transition, the crystal symmetry has been changed from monoclinic to triclinic, which accompanied massive stress accumulation within the crystal. According to our polarized optical microscope data, the α-phase of BNDI shows mechanical responses such as bending, jumping, cracking, and splitting upon heating. This thermally induced phase transition could be very useful in microelectronic devices. As a proof of principle, we used the force generated by this thermally driven phase transition to lift a metal ball nearly two orders of magnitude heavier than the crystal itself. Further, the notion that polymorphs of naphthalene diimides—an important class of organic semiconducting materials—are thermo-mechanically sensitive, with each polymorph showing distinct solid state behavior, could have important implications for the fields of organic semiconductors, optoelectronics, molecular machines, and novel chemical supramolecular bonding phenomena.

We thank Prof. M. C. Biewer and Dr H. Nyugen assistance with collecting hot stage polarized optical microscopy data. J. J. G. acknowledges the ACS-PRF (57627-DNI10) and the NSF (DMR-1654405) and M. A. O. thanks the Welch Foundation (B-1542) and NSF (CHE-1413641) for funding.

Conflicts of interest

There are no conflicts to declare.

References

1 Y. Yu, M. Nakano and T. Ikeda, *Nature*, 2003, **425**, 145.
2 E. Smela, *Adv. Mater.*, 2003, **15**, 481–494.
3 G. M. Spinks, G. G. Wallace, L. S. Fifield, L. R. Dalton, A. Mazzoldi, D. De Rossi, I. I. Khayrullin and R. H. Baughman, *Adv. Mater.*, 2002, **14**, 1728–1732.
4 R. H. Baughman, *Science*, 1999, **284**, 1340–1344.
5 R. Pelrine, *Science*, 2000, **287**, 836–839.
6 M. H. Li, P. Keller, B. Li, X. Wang and M. Brunet, *Adv. Mater.*, 2003, **15**, 569–572.
7 A. Natansohn and P. Rochon, *Chem. Rev.*, 2002, **102**, 4139–4176.
8 S. Li, M. Dharmarwardana, R. P. Welch, Y. Ren, C. M. Thompson, R. A. Smaldone and J. J. Gassensmith, *Angew. Chem.*, 2016, **55**, 10691–10696.
9 Z. Chen, N. Li, S. Li, M. Dharmarwardana, A. Schlimme and J. J. Gassensmith, *Wiley Interdiscip. Rev.: Nanomed. Nanobiotechnol.*, 2016, **8**, 512–534.
10 Z. Chen, N. Li, L. Chen, J. Lee and J. J. Gassensmith, *Small*, 2016, **12**, 4563–4571.
11 F. Terao, M. Morimoto and M. Irie, *Angew. Chem.*, 2012, **51**, 901–904.
12 S. Kobatake, S. Takami, H. Muto, T. Ishikawa and M. Irie, *Nature*, 2007, **446**, 778–781.
13 M. Lusi and J. Bernstein, *Chem. Commun.*, 2013, **49**, 9293–9295.
14 M. K. Panda, T. Runcevski, A. Husain, R. E. Dinnebier and P. Naumov, *J. Am. Chem. Soc.*, 2015, **137**, 1895–1902.
15 R. Medishetty, S. C. Sahoo, C. E. Mulijanto, P. Naumov and J. J. Vittal, *Chem. Mater.*, 2015, **27**, 1821–1829.
16 G. Liu, J. Liu, X. Ye, L. Nie, P. Gu, X. Tao and Q. Zhang, *Angew. Chem.*, 2017, **56**, 198–202.
17 Z. Chen, C. Majidi, D. J. Srolovitz and M. Haataja, *Appl. Phys. Lett.*, 2011, **98**, 011906.
18 N. K. Nath, M. K. Panda, S. C. Sahoo and P. Naumov, *CrystEngComm*, 2014, **16**, 1850.
19 A. Pathigoolla and K. M. Sureshan, *Angew. Chem.*, 2014, **53**, 9522–9525.
20 J. W. Lauher, F. W. Fowler and N. S. Goroff, *Acc. Chem. Res.*, 2008, **41**, 1215–1229.
21 Z. Li, F. W. Fowler and J. W. Lauher, *J. Am. Chem. Soc.*, 2009, **131**, 634.
22 A. Pathigoolla, R. G. Gonnade and K. M. Sureshan, *Angew. Chem.*, 2012, **51**, 4362–4366.
23 L. J. Barbour, *Aust. J. Chem.*, 2006, **59**, 595.
24 P. Naumov, S. Chizhik, M. K. Panda, N. K. Nath and E. Boldyreva, *Chem. Rev.*, 2015, **115**, 12440–12490.
25 I. Burgert and P. Fratzl, *Philos. Trans. R. Soc., A*, 2009, **367**, 1541–1557.
26 V. Balzani, A. Credi, F. M. Raymo and J. F. Stoddart, *Angew. Chem.*, 2000, **39**, 3348–3391.
27 M. Morimoto and M. Irie, *J. Am. Chem. Soc.*, 2010, **132**, 14172–14178.
28 J. J. Reczek, K. R. Villazor, V. Lynch, T. M. Swager and B. L. Iverson, *J. Am. Chem. Soc.*, 2006, **128**, 7995–8002.
29 T. Yuan, M. Vazquez, A. N. Goldner, Y. Xu, R. Contrucci, M. A. Firestone, M. A. Olson and L. Fang, *Adv. Funct. Mater.*, 2016, **26**, 8566.
30 T. Yuan, M. Vazquez, A. N. Goldner, Y. Xu, R. Contrucci, M. A. Firestone, M. A. Olson and L. Fang, *Adv. Funct. Mater.*, 2016, **26**, 8604–8612.
31 X. Hou, C. Ke, C. J. Bruns, P. R. McGonigal, R. B. Pettman and J. F. Stoddart, *Nat. Commun.*, 2015, **6**, 6884.
32 R. Rybakiewicz, I. Tszydel, J. Zapala, L. Skorka, D. Wamil, D. Djurado, J. Pecaut, J. Ulanski, M. Zagorska and A. Pron, *RSC Adv.*, 2014, **4**, 14089–14100.
33 J. Yin, K. Chaitanya and X.-H. Ju, *Can. J. Chem.*, 2015, **93**, 740–748.
34 T. He, M. Stolte, C. Burschka, N. H. Hansen, T. Musiol, D. Kalblein, J. Pflaum, X. Tao, J. Brill and F. Wurthner, *Nat. Commun.*, 2015, **6**, 5954.
35 W. Pisula, M. Kastler, D. Wasserfallen, J. W. Robertson, F. Nolde, C. Kohl and K. Mullen, *Angew. Chem.*, 2006, **45**, 819–823.
36 E. Schab-Balcerzak, A. Iwan, M. Grucela-Zajac, M. Krompiec, M. Podgorna, M. Domanski, M. Siwy and H. Janeczek, *Synth. Met.*, 2011, **161**, 1660–1670.
37 F. Würthner, C. Thalacker, S. Diele and C. Tschierske, *Chem. – Eur. J.*, 2001, **7**, 2245–2253.
38 B. Stempfle, A. Grosse, B. Ferse, K. F. Arndt and D. Woll, *Langmuir*, 2014, **30**, 14056–14061.
39 This claim is made to the best of our knowledge and a good-faith effort was put forward to identify reports to this effect. To establish this claim we conducted a series of searches between (1st of August 2016 to 5th of June 2017). The search terms and parameters used to define novelty are outlined in the ESI†.
40 E. Nauha, P. Naumov and M. Lusi, *CrystEngComm*, 2016, **18**, 4699–4703.
41 Ž. Skoko, S. Zamir, P. Naumov and J. Bernstein, *J. Am. Chem. Soc.*, 2010, **132**, 14191–14202.
42 S. Chandra Sahoo, N. K. Nath, L. Zhang, M. H. Semreen, T. H. Al-Tel and P. Naumov, *RSC Adv.*, 2014, **4**, 7640.
43 T. Shima, T. Muraoka, N. Hoshino, T. Akutagawa, Y. Kobayashi and K. Kinbara, *Angew. Chem.*, 2014, **126**, 7301–7306.
44 T. Siegrist, C. Besnard, S. Haas, M. Schiltz, P. Pattison, D. Chernyshov, B. Batlogg and C. Kloc, *Adv. Mater.*, 2007, **19**, 2079–2082.
45 S. Ghosh, M. K. Mishra, S. Ganguly and G. R. Desiraju, *J. Am. Chem. Soc.*, 2015, **137**, 9912–9921.
46 M. Horie, Y. Suzaki, D. Hashizume, T. Abe, T. Wu, T. Sassa, T. Hosokai and K. Osakada, *J. Am. Chem. Soc.*, 2012, **134**, 17932–17944.
47 P. Commins, I. T. Desta, D. P. Karothu, M. K. Panda and P. Naumov, *Chem. Commun.*, 2016, **52**, 13941–13954.
48 W. K. Ng, J. W. Kwek, A. Yuen, C. L. Tan and R. Tan, *AAPS PharmSciTech*, 2010, **11**, 159–167.
49 A. A. Van Dooren and B. W. Müller, *Thermochim. Acta*, 1982, **54**, 115–129.
50 Color changes in response to temperature in BNDI are clear indications of bandgap changes within this semiconducting material. This is quite curious and this behavior, and a full solid-state and computational analysis of it, will be followed up in a subsequent publication.